Comparison of the quasielastic $(e, e'p)$ and the (γ, p) reactions

D. G. Ireland and G. van der Steenhoven

Nationaal Instituut voor Kernfysica en Hoge-Energiefysica (NIKHEF-K),
P.O. Box 41882, 1009 DB Amsterdam, The Netherlands
(Received 14 October 1993)

Recent data obtained with the quasielastic $(e, e'p)$ reaction, and the (γ, p) reaction at photon energies of about 60 MeV, on ^{12}C, ^{16}O, ^{27}Al, ^{40}Ca, and ^{51}V are examined. Comparisons are made using distorted-wave impulse-approximation calculations. The $(e, e'p)$ data are used to determine the values of spectroscopic factors and root-mean-square radii of the overlap wave function for each transition considered. These parameters constrain the direct-knockout (DKO) calculations for the (γ, p) reactions which have been performed within the same framework. While the calculations give a very good description of the $(e, e'p)$ data, a discrepancy of typically a factor of six is observed between the DKO calculations and the (γ, p) data. The discrepancy is largely removed when meson exchange current contributions in the (γ, p) reaction are estimated on the basis of the Siegert theorem.

I. INTRODUCTION

In the quasielastic region, the $(e, e'p)$ reaction involves the emission of a proton induced by the exchange of a virtual photon. Since the (γ, p) reaction is also induced by the electromagnetic interaction, it is of interest to compare results obtained with the two reactions. We restrict this comparison to photon energies in the region 60–100 MeV in order to avoid complications due to the excitation of giant resonances or the photoproduction of pions. However, even with this limitation the mechanism of the quasielastic $(e, e'p)$ reaction, and the (γ, p) reaction need not be the same. For example, differences may be expected due to the polarization of the (virtual) photon which, in the kinematics typically employed in the experiments, is purely transverse in the (γ, p) reaction, as opposed to being predominantly longitudinal in the $(e, e'p)$ reaction. In addition, the momentum transfer $\mathbf{q}$ involved in both reactions is also considerably different: $|\mathbf{q}_{ee'p}| \sim 250$–$450$ MeV/c and $|\mathbf{q}_{\gamma p}| \sim 60$ MeV/c. These differences could result in a different sensitivity of both reactions to the nuclear currents, such as those associated with meson exchange.

It is the purpose of the present paper to perform a detailed comparison between the $(e, e'p)$ and (γ, p) reactions, making use of recently acquired high-resolution data for both reactions. The comparisons will be carried out in the framework of the direct-knockout (DKO) model, which is known to work remarkably well for the $(e, e'p)$ reaction in the quasielastic domain [1]. In this model it is assumed that a single (virtual) photon couples to a single (quasifree) nucleon in the nucleus, which is subsequently emitted into the continuum, with distortion due to final-state interactions (FSI). Using sophisticated distorted-wave impulse-approximation (DWIA) codes [2] it has been possible to extract accurate spectroscopic factors and proton momentum distributions for many nuclear orbitals from the $(e, e'p)$ data [3].

While the mechanism of the $(e, e'p)$ reaction is well understood, the mechanism of the (γ, p) reaction is still under debate. Some authors claim that DKO is the dominant mechanism describing the (γ, p) reaction (for $E_\gamma \approx$ 60–100 MeV) [4–10], while others argue that the (γ, p) reaction is dominated by meson exchange current (MEC) effects [11–13].

An important argument in favor of a DKO model is the apparent scaling of the (γ, p) data with missing momentum [4,5]. (In the plane-wave impulse-approximation the missing momentum, $\mathbf{p}_m$, can be identified with the initial momentum of the proton.) However, as a counterargument, a comparison of the (γ, p) and (γ, n) cross sections has been mentioned [14,15]. In a DKO framework, the ratio of (γ, p) to (γ, n) cross sections should be about a factor of 10. The actual observation is that the two cross sections are of comparable magnitude, which can only be explained in models involving meson exchange currents (MEC's). In fact, several theoretical groups are able to reproduce some of the existing (γ, p) and (γ, n) data using models that include MEC contributions [11–13]. However, the calculations by Gari and Hebach [11], for instance, do not properly treat the DKO part, while the random phase approximation calculations of Ryckebusch *et al.* [12], Cavinato *et al.* [13], and others do not include all aspects of the final-state interaction.

Following the large increase of high quality data both from $(e, e'p)$ and (γ, p) experiments in the last few years, we believe that it is pertinent to carry out a systematic analysis of the problem. Apart from contributing to the ongoing debate on the mechanism of the (γ, p) reaction, our work is also motivated by the growing interest in the high-momentum part of the nucleon wave function [16–18]. The relatively low spectroscopic factors deduced from recent $(e, e'p)$ data have been interpreted as evidence of short-range correlations (SRC) in nuclei [19–21]. Such effects should also reveal themselves in additional high-momentum components, which will be probed in the high missing momenta accessible in forthcoming $(e, e'p)$ experiments at new high-duty factor electron scattering facilities. However, if the (γ, p) reaction

can be understood in a DKO framework, existing (γ,p) data could already provide valuable information on possible high-momentum components, since the $\mathbf{p}_m$ range probed (300–450 MeV/c) covers the region where such effects might show up. On the other hand, if the (γ,p) reaction is dominated by MEC contributions, the existing (γ,p) data are equally valuable as a probe of MEC contributions at high missing momentum. In this respect it has to be realized that a proper interpretation of the $(e,e'p)$ data at high $\mathbf{p}_m$ also requires a good understanding of MEC effects, although they are expected to be relatively small in the $(e,e'p)$ case [22].

In the present paper, a range of nuclei is examined for which both $(e,e'p)$ and (γ,p) data (of sufficient quality to study specific transitions) exist. By analyzing the $(e,e'p)$ data in the DWIA framework, it is possible to deduce the spectroscopic factors and radial extensions of the overlap wave functions, which constrain (γ,p) calculations performed within the same framework. The comparison between the data and this calculation will immediately quantify the importance of the DKO mechanism in the (γ,p) reaction.

In the past, Findlay and Owens [4] have compared the $(e,e'p)$ and (γ,p) reactions in the kinematical domain we are presently considering. They corrected both the $(e,e'p)$ and (γ,p) data for FSI effects using a crude optical-model description, and concluded that the resulting corrected data scaled with missing momentum. This was taken to support the DKO interpretation of the (γ,p) reaction. Our approach is an improvement in various aspects: (1) A phenomenological treatment of FSI effects, which is derived from proton scattering data, is used for both reactions. (2) Antisymmetrization and orthogonality are included in the (γ,p) calculations. (3) Electron distortion effects are included in the $(e,e'p)$ calculations. (4) The parameters of the bound-state wave function are experimentally determined from the $(e,e'p)$ data. (5) The A dependence is studied. (6) An estimate of MEC effects is considered. In view of these differences, and the new high-resolution data available, our analysis can be expected to yield a more reliable comparison.

In Sec. II the method of comparing the $(e,e'p)$ and (γ,p) reaction is outlined. Section III describes the experimental data, Sec. IV the calculations. A discussion of the results is given in Sec. V, followed by a discussion of the role of MEC contributions in the (γ,p) reaction in Sec. VI. The paper is concluded with a summary and outlook.

II. METHOD OF COMPARISON

In one-nucleon removal experiments, one can define the quantities missing energy, E_m, and missing momentum, $\mathbf{p}_m$, in the following manner:

$$\mathbf{p}_m = \mathbf{p}' - \mathbf{q},$$

$$E_m = \omega - T_p - T_{A-1},$$

where $\mathbf{p}'$ and T_p are the momentum and kinetic energy

of the outgoing proton, and T_{A-1} is the kinetic energy of the residual nucleus. In the case of the $(e,e'p)$ reaction, $\mathbf{q}$ and ω are the momentum and energy transfer of the virtual photon, which can be varied independently. In the (γ,p) case, where we have $|\mathbf{q}| = \omega = E_\gamma$ (the incident photon energy), there is less kinematic freedom, resulting in relatively high $\mathbf{p}_m$ values being probed, i.e., $|\mathbf{p}_m| > 200$ MeV/c for $E_\gamma = 60$ MeV.

In the plane-wave impulse-approximation (PWIA), the $(e,e'p)$ cross section for a transition to a specific state in the residual nucleus is fivefold differential, and has a factorized form:

$$\sigma_{ee'p} \equiv \frac{d^5\sigma}{d\Omega_e d\Omega_p dE_p} = K\sigma_{ep}|\phi_\alpha(\mathbf{p}_m)|^2, \qquad (1)$$

where K is a kinematic factor $(K = \mathbf{p}'E_p)$, σ_{ep} is the off-shell electron-proton scattering cross section [23], and $\phi_\alpha(\mathbf{p}_m)$ is the overlap wave function in momentum space labeled by the quantum numbers α. Usually $\phi_\alpha(\mathbf{p}_m)$ is approximated by a single-particle bound-state wave function.

Distortion of the electron and outgoing proton waves destroys the factorization in Eq. (1), but it is still useful to define a *reduced* cross section:

$$\rho_{ee'p}(\mathbf{p}_m) = \frac{\sigma_{ee'p}}{K\sigma_{ep}}, \qquad (2)$$

where $\sigma_{ee'p}$ is the measured cross section, and the dependence on electron kinematics is to a large extent taken care of in the factor $K\sigma_{ep}$. The quantity $\rho_{ee'p}(\mathbf{p}_m)$ (which in PWIA reduces to the squared Fourier transform of the radial overlap wave function) can then be regarded as the proton momentum distribution modified by distortions and kinematics.

In the (γ,p) reaction, a PWIA factorized cross section is also obtained for the DKO model (again selecting a specific transition):

$$\sigma_{\gamma p} \equiv \frac{d\sigma}{d\Omega} = C \left(\mathbf{p}'^2_{\text{c.m.}} \sin^2\theta_p + \frac{1}{2}g_p^2\mathbf{q}^2 \right) |\phi_\alpha(\mathbf{p}_m)|^2,$$

$$(3)$$

where θ_p is the outgoing proton angle, $\mathbf{p}'_{\text{c.m.}}$ is the center-of-mass value of the outgoing proton momentum, g_p is the anomalous proton magnetic moment, and C is a kinematic factor defined as

$$C = 2\pi^2 \left(\frac{e^2}{\hbar c} \right) \left(\frac{\mathbf{p}'E_p}{(mc^2)^2} \right) \left(\frac{(\hbar c)^2}{\mathbf{q}} \right).$$

The first term between the braces in Eq. (3) is due to the coupling to the convection current, and the second represents the magnetic coupling.

By analogy with the $(e,e'p)$ case, one can also define a *reduced* cross section for the (γ,p) case:

$$\rho_{\gamma p}(\mathbf{p}_m) = \frac{\sigma_{\gamma p}}{C \left(\mathbf{p}'^2_{\text{c.m.}} \sin^2\theta_p + \frac{1}{2}g_p^2\mathbf{q}^2 \right)}. \qquad (4)$$

It can be seen from Eqs. (1) and (3) that in PWIA the reduced cross sections should be identical:

$$\rho_{ee'p} = \rho_{\gamma p} = |\phi_\alpha(\mathbf{p}_m)|^2.$$

To date, the $(e, e'p)$ data have sampled low $\mathbf{p}_m$ ($<$ 250 MeV/c), while the (γ, p) data have sampled somewhat higher values ($\mathbf{p}_m > 250$ MeV/c). It may be argued that, in the DKO framework, the two measurements are complementary in the sense that they measure the same momentum distribution, but at different $\mathbf{p}_m$. Therefore, both $(e, e'p)$ and (γ, p) reduced cross sections would be expected to scale as a function of $\mathbf{p}_m$ if DKO is a good description of the (γ, p) mechanism.

In the present work, we make no *a priori* assumption as to the (γ, p) reaction mechanism. The reason for using the reduced cross-section representation is that it enables us to show the $(e, e'p)$ and (γ, p) data on the same scale, which would not be possible with a cross-section representation. Note that, for comparisons with calculations, as long as both the data and the calculations are divided by the same factor, any representation is valid.

III. EXPERIMENTAL DATA

In comparing the $(e, e'p)$ and (γ, p) reactions, recent high-resolution data obtained on five nuclei (^{12}C, ^{16}O, ^{27}Al, ^{40}Ca, and ^{51}V) were used. We only considered nuclei where the DWIA formalism is expected to provide a reasonable approximation of the FSI, since the distorting optical-model potentials have been derived from the analysis of proton scattering experiments. The largest possible range of A was selected [subject to the availability of adequate $(e, e'p)$ and (γ, p) data] in order to demonstrate which features appear to be common to reactions of this type. In addition, the transitions chosen are all below the two-particle emission threshold in the residual nuclei. Effects seen beyond this threshold, while interesting in their own right both for $(e, e'p)$ and (γ, p) [24,25,20,26], are beyond the scope of the present paper.

As the subject of this paper is the comparison between the two different reactions, we shall only briefly describe the experiments themselves. In almost all cases the data used have been published elsewhere, and therefore we refer to the original publications for more detailed information.

All the $(e, e'p)$ data [27,24,28–31] were taken at the NIKHEF-K facility. The electron beam had a duty factor of typically 1% and energies between 280 and 480 MeV. The use of the dispersion-matching technique and a high-resolution spectrometer pair [32] made it possible to obtain a missing energy resolution in the range 100–200 keV. All measurements used in the present analysis were performed in parallel kinematics [i.e., $\mathbf{p}'$ either parallel ($|\mathbf{p}'| > |\mathbf{q}|$) or antiparallel ($|\mathbf{p}'| < |\mathbf{q}|$) to $\mathbf{q}$]. The outgoing proton kinetic energy, T_p, was 70 MeV for ^{12}C$(e, e'p)$, 96 MeV for ^{16}O$(e, e'p)$, and 100 MeV for ^{27}Al$(e, e'p)$ and ^{40}Ca$(e, e'p)$. The ^{51}V$(e, e'p)$ measurements were carried out at $T_p = 70$ and 100 MeV. The cross sections were determined with a systematic uncertainty of about 5%. An exception to this was the ^{27}Al,$(e, e'p)$ data [29], which were taken during the very first $(e, e'p)$ runs at the NIKHEF-K facility. The uncertainty in this data is 15%,

which has been included in the error bars.

The high-resolution (γ, p) data for ^{12}C, ^{27}Al, and ^{51}V [33] were taken at the MAXLAB photon tagging facility in Lund, Sweden [34] using a silicon strip/hyperpure germanium detector system for protons. We note in passing that the ^{12}C and ^{27}Al(γ, p) data taken from Ref. [33] are by no means unique, and that previous measurements at other laboratories also exist [35–39]. These measurements are consistent at the level of the systematic uncertainties [39]. The ^{40}Ca(γ, p) data were also obtained at the MAXLAB facility, using a different silicon/germanium proton detection system [40]. Finally, data for the reaction ^{16}O(γ, p) was obtained using a bremsstrahlung difference method [41]. All (γ, p) data were taken with a photon energy of about 60 MeV. The typical systematic uncertainty in the (γ, p) data is 20%.

High quality (γ, p) data taken at a photon energy of about 80 MeV are also available. Exploratory calculations have shown that the conclusions obtained in this paper also apply to the 80 MeV (γ, p) data. For that reason the 80 MeV data will not be considered any further.

IV. CALCULATIONS

The calculations used to describe the $(e, e'p)$ data are based upon the work by the Pavia group [42–46,2]. They use a model which employs a nonrelativistic one-body off-shell current operator, nonrelativistic bound-state wave functions, and a partial wave expansion to calculate the distortion of the outgoing proton waves, using a nonrelativistic optical-model potential. Electron distortion is also taken into account, and the resulting calculations are known as a complete distorted-wave impulse-approximation (CDWIA) analysis [45,46].

Several checks were performed to evaluate the validity of the CDWIA calculations. The calculated phase shifts are in agreement with those produced by proton scattering distorted-wave Born approximation (DWBA) codes. The code was also run to compare DWIA calculations with distorting potential depths were set to zero, to PWIA calculations obtained analytically. The two calculations were found to agree on the 10^{-3} level over the entire range of missing momenta appropriate to the present study.

The optical-model potentials were chosen to be the same as those used in the original analyses [27,24,28–31]. For ^{12}C the optical-model of Comfort and Karp [47] was used. All others employed the optical-model of Schwandt *et al.* [48]. Both potentials were obtained by fits to proton scattering data, and are parametrized as functions of the outgoing proton kinetic energy.

The bound-state wave functions were calculated by solving the Schrödinger equation for Woods-Saxon potential wells. The diffuseness parameter, a_0, was kept constant at 0.65 fm in all cases, since calculations appear to be insensitive to variations of it. In order to obtain a good description of the $(e, e'p)$ data, both the root-mean-square radius ($r_{\rm rms}$) of the bound-state wave function and the spectroscopic factor (S_α) were fitted.

The results of such fits have already been presented in the original publications, but as several modifications of the code have been implemented since the original analyses, all fits had to be repeated. Electron distortion is now evaluated in a more sophisticated manner [45,46], an error in the nonlocality correction has been removed and the center-of-mass value of the outgoing proton momentum is calculated nonrelativistically in order to be consistent with the nonrelativistic character of the calculation.

In Table I we list the various parameters for each transition which were found in the present analysis. The new values for r_{rms} and S_α listed in Table I differ by no more than 2% and 5%, respectively, from the values quoted in the original publications. Hence, the conclusions drawn in those papers are not affected. In the case of ^{12}C, the parameter η was also used to be consistent with the analysis of Ref. [27] where it was introduced to account for a transverse enhancement in the data. [In this analysis the transverse response function was multiplied by η^2, i.e., the parameter η is a measure of the relative enhancement of the transverse $(e,e'p)$ response compared to the longitudinal response.] It should be noted that the quoted values of r_{rms} and S_α for the three p-shell transitions in ^{12}C include a correction for coupled-channel effects, using the prescription in Ref. [27].

The data for ^{27}Al$(e,e'p)$ were neither of sufficient accuracy nor of sufficient range in p_m to deduce values of r_{rms}. Instead, we have used a value of r_{rms} which was obtained using magnetic elastic electron scattering [49]. We have assumed a 10% uncertainty on this value of r_{rms}.

Turning now to the (γ,p) calculations, these were again based on the work of Boffi et $al.$ [6,7], and have the advantage of being performed within the same framework as those of $(e,e'p)$. In addition to the nonrelativistic calculation of DKO, the calculations include several other ingredients. A correction is applied to the proton continuum wave function in order to restore orthogonality and antisymmetry, which are destroyed when one uses an optical-model potential which differs from that used to calculate bound-state wave functions. At low p_m [the $(e,e'p)$ regime], this correction is not significant, but at higher values [those commensurate with (γ,p)], it does have an important effect [7].

The orthogonalization-antisymmetrization (OA) correction is applied to the final-state wave function by explicitly evaluating the nonzero overlap with all occupied single-particle wave functions, ϕ_α. To apply the OA correction properly, a set of wave functions ϕ_α must be generated that form an orthonormal set. We can ensure this by calculating, for a given transition, all wave functions with the same Woods-Saxon potential that was used to evaluate the bound-state wave function fitted to the $(e,e'p)$ data. In general, therefore, each separate transition will have a distinct set ϕ_α corresponding to the binding energy and r_{rms} of that transition.

A nonlocality correction is not applied to the continuum wave function in the (γ,p) case since, as was argued in Ref. [50], the application of both the OA and nonlocality corrections would amount to double counting. Furthermore, the correction due to the coupling of the photon to the current of the $A-1$ system is not applied

TABLE I. The values of r_{rms} and S_α extracted in the present analysis.

Target nucleus	Final state J^π	E_x (MeV)	r_{rms} (fm)	η	S_α
^{12}C	$\frac{3}{2}^-$	0.000	2.806(37)	1.107(39)	1.825(33)
	$\frac{1}{2}^-$	2.125	2.958(43)	1.193(59)	0.275(10)
	$\frac{3}{2}^-$	5.020	2.871(48)	1.164(67)	0.217(10)
	$\frac{7}{2}^{-a}$	6.743	4.295	1.00	0.0038(10)
	$\frac{1}{2}^+$	6.792	3.527	1.00	0.0084(6)
	$\frac{5}{2}^+$	7.286	3.525	1.61(3)	0.014(1)
^{16}O	$\frac{1}{2}^-$	0.000	2.923(111)	–	1.124(61)
^{27}Al^b	2^+	1.81	3.254	–	0.347(38)
	2^+	4.33	3.254	–	0.707(91)
^{40}Ca	$\frac{3}{2}^+$	0.000	3.667(26)	–	2.698(44)
^{51}V	0^+	0.000	4.197(33)	–	0.384(8)
	2^+	1.554	4.189(52)	–	0.165(5)
	4^+	2.675	4.194(29)	–	0.346(6)
	6^+	3.199	4.218(32)	–	0.514(10)

^{a} The complex at $\sim$7 MeV in ^{12}C(γ,p) is a special case, and is treated as an incoherent sum of the three $(\frac{7}{2}^-, \frac{1}{2}^+, \frac{5}{2}^+)$ states. We have used the r_{rms} values from Ref. [24] and re-fitted spectroscopic factors.

^{b}The r_{rms} values were taken from [49], and the S_α's fitted. An 10% error was assumed for r_{rms} for the subsequent (γ,p) calculations.

(in contrast to Ref. [50]), because it represents a contribution in addition to DKO. As the aim of this study is to make a consistent comparison of $(e, e'p)$ and (γ, p) reactions within a quasielastic DKO framework, it must be omitted. There is also some ambiguity in the evaluation of this correction. We note, however, that the application of the correction does not make any difference to the general features of this work.

In all cases the bound-state wave functions used as input to the (γ, p) DKO calculations were obtained from the $(e, e'p)$ CDWIA analysis, and the optical potentials used were the same parametrizations (taking into account the difference in kinetic energy of the outgoing proton).

The (γ, p) DKO calculation was also checked for consistency. The phase shifts were found to agree with those evaluated using the $(e, e'p)$ CDWIA code on the 10^{-2} level. Furthermore, a check was made that the kinematics were evaluated in a similar, nonrelativistic fashion.

V. DISCUSSION

The data described in Sec. II, and the calculations described in Sec. III have been collated and are depicted in Figs. 1–3. The $(e, e'p)$ data are shown as black circles,
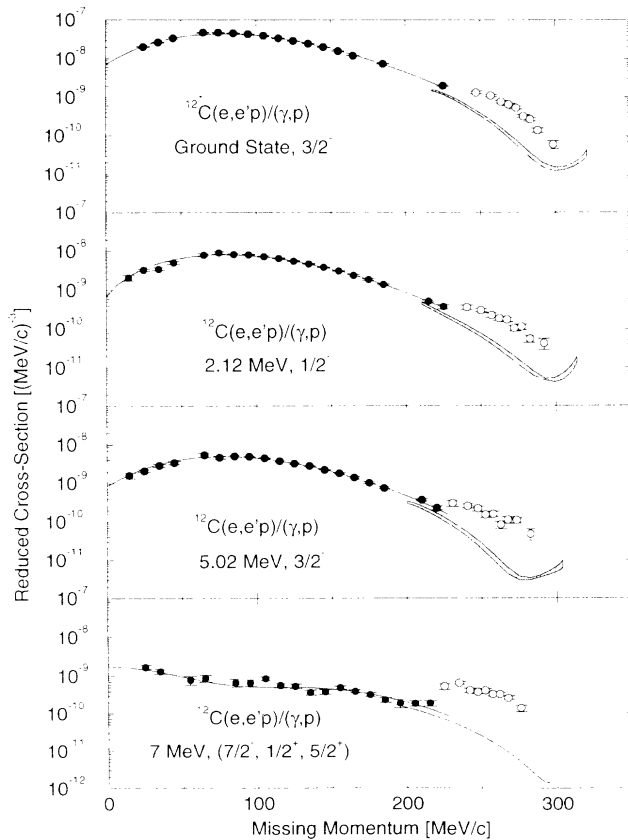
FIG. 1. $^{12}C(e, e'p)$ and (γ, p) data plotted in terms of reduced cross sections as a function of the missing momentum. The black (open) circles represent the $(e, e'p)$ data [(γ, p) data]. The solid line represents the CDWIA calculation for the $(e, e'p)$ reaction, and the shaded error band the corresponding DKO-DWIA calculation for the (γ, p) reaction.
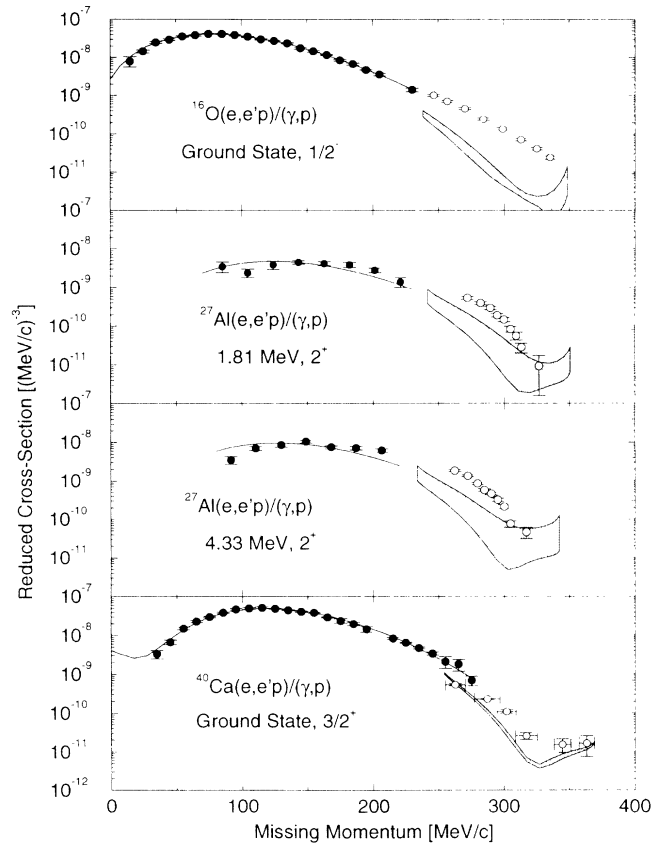
FIG. 2. Selected transitions for proton knockout from the nuclei ^{16}O, ^{27}Al, and ^{40}Ca. The points and curves have the same meanings as in Fig. 1.
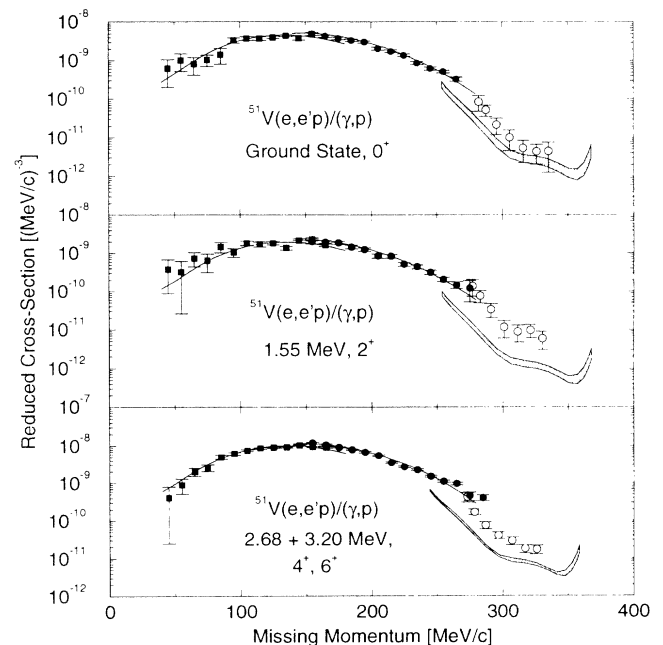
FIG. 3. The $1f_{7/2}$ transitions for proton knockout from ^{51}V. The points and curves have the same meanings as in Fig. 1. Note that in the third panel the sum of two transitions is shown.

and only $|\mathbf{p}'| > |\mathbf{q}|$ points are shown since $|\mathbf{p}'| < |\mathbf{q}|$ points do not add to the information obtained. For ^{51}V in Fig. 3 the black squares (circles) represent $T_p = 70$ (100) MeV. The (γ,p) data are shown as the open circles. The solid line through the $(e,e'p)$ points represents the CDWIA calculation and the shaded band represents the DKO (γ,p) calculation when the uncertainty in the fitted parameters extracted from the CDWIA analysis is taken into account. The error due to uncertainties in the optical potential is not included.

A general observation is that while the $(e,e'p)$ and (γ,p) data appear superficially to scale as a function of $\mathbf{p}_m$, most transitions do not show a smooth overlap when examined in detail. The differences between the (γ,p) and $(e,e'p)$ data in the overlap region also vary considerably for each transition. Hence we do not find evidence for universal scaling in this kinematic domain. Another observation is that in all cases, the $(e,e'p)$ data are well described, while the DKO calculation does not equal the (γ,p) data, and is always smaller. Note that as a result of differences of the FSI between the two reactions, a discontinuity arises going from $(e,e'p)$ to (γ,p) calculations.

Looking in detail at ^{12}C (Fig. 1), it can be seen that the three transitions corresponding to knockout from the p shell all behave in a similar fashion. The data corresponding to the peak at $E_x = 7$ MeV are seen to have a somewhat different character. These data represent three unresolved states in ^{11}B which correspond to $1f$, $2s$, and $1d$ knockout in a DKO framework [24]. In this case the data do not come close to scaling. The data for this peak are enhanced by a factor of 2 compared to other transitions. The observation that this peak has apparently enhanced strength when missing energy spectra from the two reactions are compared has been the subject of previous publications [36,51,50,52]. The DKO calculation represents the incoherent sum of contributions of knockout from the $1f_{7/2}$, $2s_{1/2}$, and $1d_{5/2}$ shells. It is represented by a single line as r_{rms} has not been obtained by means of a fitting procedure. More details are to be found in Ref. [24].

In Fig. 2 it can be seen that the transition from ^{16}O to the ground state of ^{15}N behaves like the transition to the $\frac{1}{2}^{-}$ state in ^{11}B. The wider error band reflects the fact that a larger error bar on r_{rms} was obtained in the CDWIA analysis.

The two ^{27}Al transitions (also in Fig. 2) show that the assumed error of 10% in the value of r_{rms} has a sizable effect on the DKO calculations. However, the observation of the DKO calculation falling below the data still holds. It would be relatively straightforward to improve the ^{27}Al$(e,e'p)$ data, which would help to decrease the width of the error band seen in the present plots.

The $1d_{5/2}$ transition for ^{40}Ca$(e,e'p)/(\gamma,p)$ displays the same general feature. The comparison of the DKO calculation to the data is less convincing due to the size of the error bars on $\mathbf{p}_m$ which are a result of an extended proton detector [40].

Figure 3 shows that all transitions attributed to $1f_{7/2}$ knockout from ^{51}V have the same character. The 4^+ and 6^+ states have been added (incoherently), since it was not possible to separate them in the (γ,p) analysis [33]. The difficulty in separating the contributions from each state in ^{51}V(γ,p) can also be seen in the fact that the 0^+ and 2^+ states have somewhat larger statistical error bars. In all ^{51}V cases, the accurate $(e,e'p)$ measurement gives a DKO error band with low uncertainty compared to the accuracy of the (γ,p) data points.

In the ^{40}Ca and ^{51}V cases, it can be seen that the DKO calculation results in an error band which is nearer the data, although definitely too low to account for it. The shapes of the curves also appear to be in better agreement with the data for these heavier nuclei.

The difference between the DKO calculations and the (γ,p) data has been quantified by taking the mean value of the error bands at each $\mathbf{p}_m$ point and calculating a ratio of data to DKO calculation for each of the selected transitions. The results are shown in Table II. The numbers are a measure of the additional strength seen in the

TABLE II. The ratios of the (γ,p) data to the DKO and the DKO plus MEC calculations for each transition (see text).

Target nucleus	Final state J^π	E_x (MeV)	Ratio of data to DKO	Ratio of data to DKO + MEC
^{12}C	$\frac{3}{2}^{-}$	0.000	4.8(0.6)	0.9(0.2)
	$\frac{1}{2}^{-}$	2.125	4.6(0.5)	0.8(0.1)
	$\frac{3}{2}^{-}$	5.020	6.0(1.2)	0.8(0.2)
	$\frac{7}{2}^{-} + \frac{1}{2}^{+} + \frac{5}{2}^{+}$	7	13.9(1.9)	—
^{16}O	$\frac{1}{2}^{-}$	0.000	7.0(1.8)	1.3(0.4)
^{27}Al	2^+	1.81	5.7(0.5)	1.5(0.2)
	2^+	4.33	6.8(0.6)	1.7(0.1)
^{40}Ca	$\frac{3}{2}^{+}$	0.000	1.4(0.3)	0.3(0.1)
^{51}V	0^+	0.000	2.7(0.6)	1.1(0.4)
	2^+	1.554	8.0(2.7)	2.6(1.0)
	$4^+ + 6^+$	2.9	3.2(0.3)	1.0(0.2)

(γ, p) data when compared to the *constrained* DKO calculations. On average the ratio amounts to 5.8, with a spread around this value as shown in the table. However, large differences are observed in particular for the 7 MeV state in ^{11}B (factor 14) and the ^{39}K ground-state transition (factor 1.4). The systematics of, and the typical size of the enhancement factor rules out the possibility that minor modifications of the DKO calculations (by taking a slightly different optical potential, for instance) could result in a good description of the (γ, p) data.

In view of the fact that an accurate CDWIA analysis of the $(e, e'p)$ data also puts tight constraints on the DKO calculations for the (γ, p) reaction, and because the effect is seen for all transitions considered, we believe that the large discrepancy shown in the present work is not an artifact of the calculations. Previous work [4–10] which argued in favor of a pure DKO description of (γ, p) data in the photon-energy domain between 60 and 100 MeV, is clearly at variance with this conclusion. We attribute this difference to the fact that in Refs. [4–8,10] the DKO calculations were not constrained by experimental information available from $(e, e'p)$ and (p, p') experiments.

VI. ESTIMATE OF MEC EFFECTS

Several authors, including Gari and Hebach [11], Ryckebusch et al. [53,12], and others have argued that MEC's play a prominent role in the (γ, p) reaction, even for photon energies below 100 MeV. In particular, the calculations of Ryckebusch et al. have been successful in describing, for instance, the ^{12}C(γ, p) data (including the "enhanced" 7 MeV peak) [52]. However, due to the complexity of these calculations, it has not been possible

up to now to apply this type of calculation to all nuclei. Moreover, as was mentioned before, many of the available theoretical calculations do not contain a fully satisfactory treatment of the DKO and/or FSI contributions.

In order to estimate the effect of MEC's in the present framework, PWIA calculations have been performed which are based on the Siegert theorem. The reason for using the Siegert theorem to estimate MEC effects stems from the deuterium photodisintegration calculations of Arenhövel [54]. He shows that an explicit calculation of MEC effects for the reaction ^{2}H(γ, p) at $E_\gamma = 60$ MeV is very close to an impulse-approximation calculation which includes the Siegert theorem. The Siegert theorem, which is based on current conservation, states that, in the long-wavelength limit, the convection current matrix element of multipolarity L may be replaced by the appropriately scaled charge matrix element [11,55]:

$$T_L^{conv}(\mathbf{q}) = \frac{E_f - E_i}{|\mathbf{q}|} \sqrt{\frac{L+1}{L}} T_L^{charge}, \qquad (5)$$

where $E_{i(f)}$ is the initial (final) energy.

It has been argued [56] that in the limit of $\mathbf{q} \to 0$, the Siegert theorem implicitly includes exchange contributions of lowest order (higher orders being negligible). We further assume the dominance of the $E1$ multipole which is known to be reasonable for photoabsorption processes [54]. In fact Gari and Hebach [11] based their evaluation of MEC contributions to (γ, p) upon similar assumptions. Our approach is different from theirs in the treatment of the DKO contributions and the FSI. Within our framework, it is possible to derive a PWIA cross-section expression which includes MEC effects [cf. Eq. (3)]:

$$\frac{d\sigma}{d\Omega} = C \left(\left(\frac{3}{2} \frac{e}{\mu_N} \right)^2 \left(\frac{\mathbf{q}}{\mathbf{p}_m} \right)^2 \left(\frac{\mathbf{p}'_{c.m.}}{\mathbf{p}_m} \right)^2 \sin^2 \theta_p + \frac{1}{2} g_p^2 \mathbf{q}^2 \right) |\phi_\alpha(\mathbf{p}_m)|^2, \qquad (6)$$

where e is the unit charge and μ_N is the nuclear magneton. Using this equation, it is straightforward to evaluate the ratio of the plane-wave plus Siegert (PWS) and PWIA cross sections for each data point. The points given by the full DKO calculation were then multiplied by the appropriate PWS/PWIA ratio. Hence, it is also assumed that the effects due to MEC and FSI can be separately treated. This is not generally true, but likely to be good enough for our purposes.

The present method is not intended to be exact; it is rather meant to be an estimate which can be performed in a relatively straightforward manner within the framework of existing DKO codes. For instance, it is clear that the arguments of Sec. IV which stressed the importance of orthogonal wave functions have now been disregarded since, in using the Siegert theorem, we have altered our Hamiltonian while retaining the original wave functions.

In Fig. 4 the results of the aforementioned estimate are shown. Only selected transitions are displayed for each nucleus (similar results are found for all transitions). As

in previous figures, the (γ, p) data are shown as open circles and the DKO calculations are represented by the lightly shaded band. The DKO+MEC calculation is represented by the dark shaded band. The transition to the 7 MeV complex in ^{12}C(γ, p) is a special case to which we shall return later.

It is clear that the MEC estimate is in much better agreement with the data than a "pure" DKO calculation. In all cases, except perhaps ^{16}O, a good agreement in magnitude and shape is found. To quantify this statement, the ratios of data to DKO+MEC calculations have been evaluated as in Sec. V, and are also given in Table II. It shows that while the data are enhanced by an average factor of 5.8 when compared to a pure DKO calculation, this factor is reduced to an average of 1.2 when MECs are included in our calculation using the Siegert theorem. This confirms the theoretical arguments of Refs. [11,52] which stress that MEC contributions dominate the (γ, p) reaction. A more refined description of the data requires a calculation which treats

MEC's explicitly, and includes long- and short-range correlations as well.

The treatment of the 7 MeV state in $^{12}\text{C}(\gamma,p)$ has followed that of Ref. [50], where it was shown that two-step processes in the excitation of the $\frac{7}{2}^-$ state contribute significantly to the magnitude of the cross section. The value of these two-step calculations was recently demonstrated in a dedicated $^{12}\text{C}(e,e'p)$ experiment at low p_m [57]. In the figure, the dotted line is the pure DKO calculation, the dashed line represents the addition of two-step processes to this, and the solid line is the result of multiplying by the PWS/PWIA ratio. The difference between this calculation and that of Ref. [50] is that here we do not include the coupling to the $A-1$ system, while we do show the effect of the MEC estimate. Clearly, the combination of two-step processes and MEC effects yields the correct order of magnitude, indicating that a treatment of two-step processes and MEC's within one consistent framework might well be able to describe the data.

A different explanation for the strong excitation of this transition has been proposed by Ryckebusch et al. [52]. The MEC's are explicitly included in a two-particle–two-hole framework in their calculation, and it reproduces the data fairly well. While the two calculations agree as to the importance of including MEC effects, there is an interesting difference. The calculation of Ryckebusch et al. finds that the excitation of the $\frac{5}{2}^+$ state is the dominant contribution to the 7 MeV peak, while in our approach the $\frac{7}{2}^-$ state is responsible for the added strength due to two-step processes. A high-resolution proton knockout measurement at high p_m might resolve this issue.

VII. SUMMARY AND OUTLOOK

It has been shown that when quasielastic $(e,e'p)$ data and (γ,p) data taken at $E_\gamma \sim 60$ MeV are plotted as reduced cross sections, scaling as a function of p_m does not occur. Calculations performed within the same DWIA framework also show discontinuities between the p_m ranges covered by the two reactions. This difference is partly attributed to FSI differences for protons of different outgoing kinetic energies.

In addition to this, the DKO calculations for the (γ,p) reaction, which have been constrained by the parameters deduced in the CDWIA analysis of the $(e,e'p)$ data, underestimate the data by a typical factor of 6 across a range of nuclei from $A=12$ to 51. Hence we believe that (γ,p) cross sections cannot be understood in a pure DKO framework. An estimate of MEC contributions based on the Siegert theorem has shown that they are significant, and that in many cases a good agreement in magnitude and shape is observed between the data and the calculation. A full treatment of the problem, which should include the effects of long- and short-range correlations as well as MEC's and the DKO contribution, is clearly required for all nuclei.

The issues presented in this paper may be further elucidated by future work. It would of great interest to compare $(e,e'p)$ and (γ,p) data at the same (high) p_m values. In which case, no uncertainty should arise due to
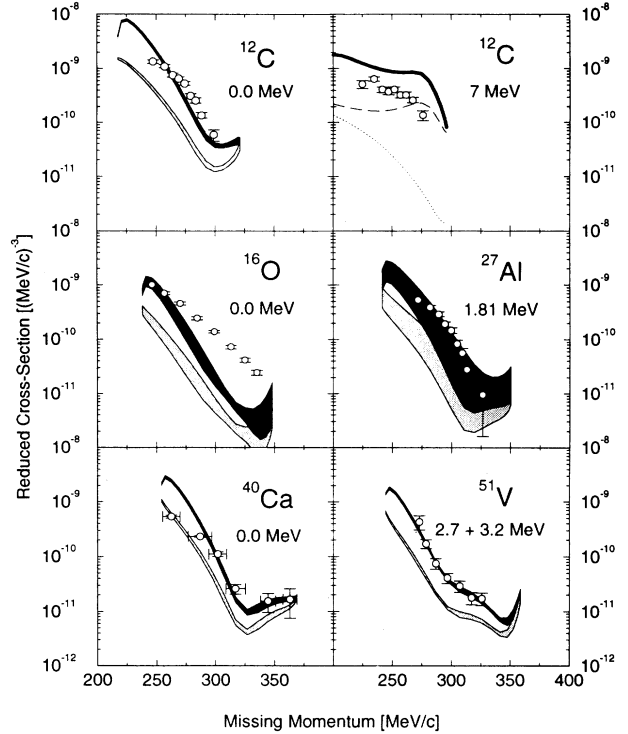

FIG. 4. The effect of applying the Siegert theorem to estimate MEC effects on some selected (γ,p) transitions. The DKO calculations are shown as light shaded bands, and the DKO+MEC calculations are represented by the darker bands. The $^{12}\text{C}(\gamma,p)$ transition to the 7 MeV complex is addressed separately in the text.

the difference in p_m range probed in the two reactions. By separating the longitudinal and transverse response in such $(e,e'p)$ measurements, it might also be possible to isolate MEC contributions in the transverse $(e,e'p)$ response, which could then be compared to the (purely transverse) (γ,p) results. We have already mentioned that a high-resolution $^{12}\text{C}(e,e'p)$ measurement at high p_m might resolve the state whose excitation is responsible for the enhanced strength of the 7 MeV complex in ^{11}B. An improved measurement of $^{27}\text{Al}(e,e'p)$ would help to reduce the uncertainty in the DKO calculation for the $^{27}\text{Al}(\gamma,p)$ reaction. It would also be of interest to extend the comparison of $(e,e'p)$ and (γ,p) data to heavy nuclei (e.g., ^{208}Pb) in order to explore the validity of our conclusions at a considerably larger nuclear mass.

ACKNOWLEDGMENTS

[1] S. Frullani and J. Mougey, Adv. Nucl. Phys. **14**, 1 (1984).

[2] S. Boffi, C. Giusti, and F.D. Pacati, Phys. Rep. **226**, 1 (1993).

[3] P.K.A. de Witt Huberts, J. Phys. G **16**, 507 (1990).

[4] D.J.S. Findlay and R.O. Owens, Nucl. Phys. **A292**, 53 (1977).

[5] D.J.S. Findlay, R.O. Owens, M.J. Leitch, J.L. Matthews, C.A. Peridier, B.L. Roberts, and C.P. Sargent, Phys. Lett. **74B**, 305 (1978).

[6] S. Boffi, C. Giusti, and F.D. Pacati, Nucl. Phys. **A359**, 91 (1981).

[7] S. Boffi, R. Cenni, C. Giusti, and F.D. Pacati, Nucl. Phys. **A420**, 38 (1984).

[8] M.J. Leitch et al., Phys. Rev. C **31**, 1633 (1985).

[9] J.L. Matthews, in *Proceedings of the Third Workshop on Perspectives in Nuclear Physics at Intermediate Energies*, ICTP, Trieste, 1987, edited by S. Boffi, C. Ciofi degli Atti, and M. Giannini (World Scientific, Singapore, 1988), p. 611.

[10] B. Hoïstad et al., Phys. Lett. B **276**, 294 (1992).

[11] M. Gari and H. Hebach, Phys. Rep. **72**, 1 (1981).

[12] J. Ryckebusch, M. Waroquier, K. Heyde, J. Moreau, and D. Ryckbosch, Nucl. Phys. **A476**, 237 (1988).

[13] M. Cavinato, M. Marangoni, and A.M. Saruis, Nucl. Phys. **A422**, 237 (1984).

[14] H. Göringer and B. Schoch, Phys. Lett. **97B**, 41 (1980).

[15] H. Göringer, B. Schoch, and G. Lührs, Nucl. Phys. **A384**, 414 (1982).

[16] Z.Y. Ma and J. Wambach, Phys. Lett. B **256**, 1 (1991).

[17] C. Mahaux and R. Sartor, Adv. Nucl. Phys. **20**, 1 (1991).

[18] W.H. Dickhoff and H. Müther, Rep. Prog. Phys. **55**, 1947 (1992).

[19] A.E.L. Dieperink and P.K.A. de Witt Huberts, Annu. Rev. Nucl. Part. Sci. **40**, 239 (1990).

[20] G. van der Steenhoven, Nucl. Phys. **A527**, 17c (1991).

[21] L. Lapikás, Nucl. Phys. **A553**, 297c (1994).

[22] M. Radici, in *Proceeding of the Workshop in Electron-Nucleus Scattering*, Elba International Physics Center, 1993 (World Scientific, Singapore, 1994).

[23] T. de Forest, Jr., Nucl. Phys. **A392**, 232 (1983).

[24] G. van der Steenhoven, H.P. Blok, E. Jans, L. Lapikás, E.N.M. Quint, and P.K.A. de Witt Huberts, Nucl. Phys. **A484**, 445 (1988).

[25] J.C. McGeorge et al., Phys. Lett. B **179**, 212 (1986).

[26] P.E. Ulmer et al., Phys. Rev. Lett. **59**, 2259 (1987).

[27] G. van der Steenhoven, H.P. Blok, E. Jans, M. de Jong, L. Lapikás, E.N.M. Quint, and P.K.A. de Witt Huberts, Nucl. Phys. **A480**, 547 (1988).

[28] M.B. Leuschner et al., Phys. Rev. C **49**, 955 (1994).

[29] E.N.M. Quint, Master's thesis, Universiteit van Amsterdam, 1983 (unpublished).

[30] G.J. Kramer, Ph.D. thesis, Universiteit van Amsterdam, 1990.

[31] J.W.A. den Herder, H.P. Blok, E. Jans, P.H.M. Keizer, L. Lapikás, E.N.M. Quint, G. van der Steenhoven, and P.K.A. de Witt Huberts, Nucl. Phys. **A490**, 507 (1988).

[32] C. de Vries, C.W. de Jager, L. Lapikás, G. Luijckx, R. Maas, H. de Vries, and P.K.A. de Witt Huberts, Nucl. Instrum. Methods **223**, 1 (1984).

[33] D.G. Ireland et al., Nucl. Phys. **A554**, 173 (1993).

[34] J-O. Adler et al., Nucl. Instrum. Methods A **294**, 15 (1990).

[35] J.L. Matthews, D.J.S. Findlay, S.N. Gardiner, and R.O. Owens, Nucl. Phys. **A267**, 51 (1976).

[36] A.C. Shotter, S.V. Springham, D. Branford, J. Yorkston, J.C. McGeorge, B. Schoch, and P. Jennewein, Phys. Rev. C **37**, 1354 (1988).

[37] S.V. Springham et al., Nucl. Phys. **A517**, 93 (1990).

[38] A. Sada et al., Nucl. Phys. **A551**, 125 (1993).

[39] L.J. de Bever, Ph.D. thesis, Universiteit van Utrecht, 1993.

[40] C. van den Abeele et al., Phys. Lett. B **296**, 302 (1992).

[41] D.J.S. Findlay and R.O. Owens, Nucl. Phys. **A279**, 385 (1977).

[42] S. Boffi, C. Giusti, and F.D. Pacati, Nucl. Phys. **A336**, 416 (1980).

[43] C. Giusti and F.D. Pacati, Nucl. Phys. **A336**, 427 (1980).

[44] S. Boffi, C. Giusti, and F.D. Pacati, Nucl. Phys. **A336**, 437 (1980).

[45] C. Giusti and F.D. Pacati, Nucl. Phys. **A473**, 717 (1987).

[46] C. Giusti and F.D. Pacati, Nucl. Phys. **A485**, 461 (1988).

[47] J.R. Comfort and B.C. Karp, Phys. Rev. C **21**, 2162 (1980).

[48] P. Schwandt, H.O. Meyer, W.W. Jacobs, A.D. Bacher, S.E. Vigdor, M.D. Kaitchuck, and T.R. Donoghue, Phys. Rev. C **26**, 55 (1982).

[49] T.W. Donnelly and I. Sick, Rev. Mod. Phys. **56**, 461 (1984).

[50] G. van der Steenhoven and H.P. Blok, Phys. Rev. C **42**, 2597 (1990).

[51] L. Van Hoorebeke et al., Phys. Rev. C **42**, R1179 (1990).

[52] J. Ryckebusch, K. Heyde, L. Machenil, D. Ryckbosch, M. Vanderhaeghen, and M. Waroquier, Phys. Rev. C **46**, R829 (1992).

[53] J. Ryckebusch, M. Waroquier, K. Heyde, and D. Ryckbosch, Phys. Lett. B **194**, 453 (1987).

[54] H. Arenhövel and M. Sanzone, *Few Body Systems* (Springer-Verlag, Vienna, 1991), Suppl. 3.

[55] A.J.F. Siegert, Phys. Rev. **52**, 787 (1937).

[56] H. Arenhövel, Z. Phys. A **302**, 25 (1981).

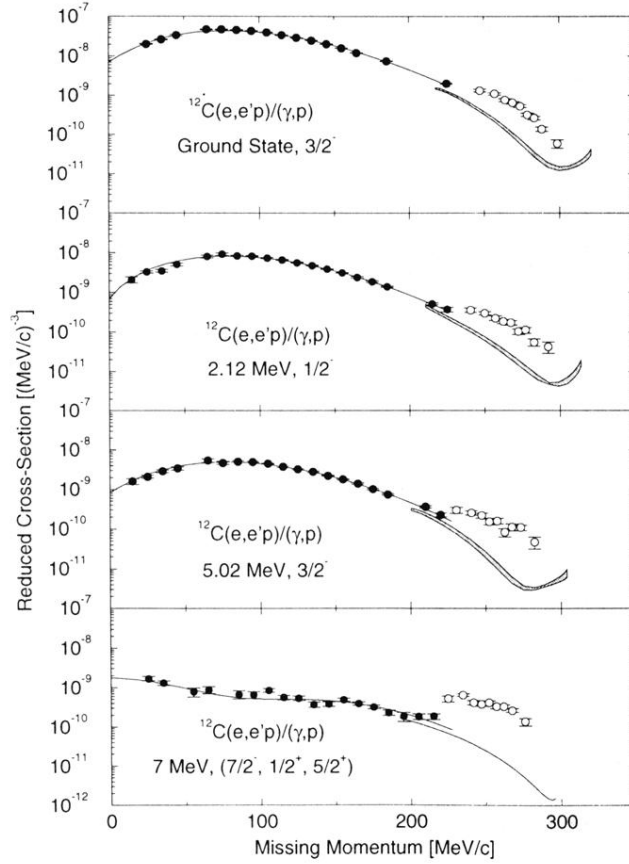[57] I. Bobeldijk, H.P. Blok, and G. van der Steenhoven, Phys. Lett. B **281**, 25 (1992).

FIG. 1. ^{12}C$(e, e'p)$ and (γ, p) data plotted in terms of reduced cross sections as a function of the missing momentum. The black (open) circles represent the $(e, e'p)$ data $[(\gamma, p)$ data]. The solid line represents the CDWIA calculation for the $(e, e'p)$ reaction, and the shaded error band the corresponding DKO-DWIA calculation for the (γ, p) reaction.
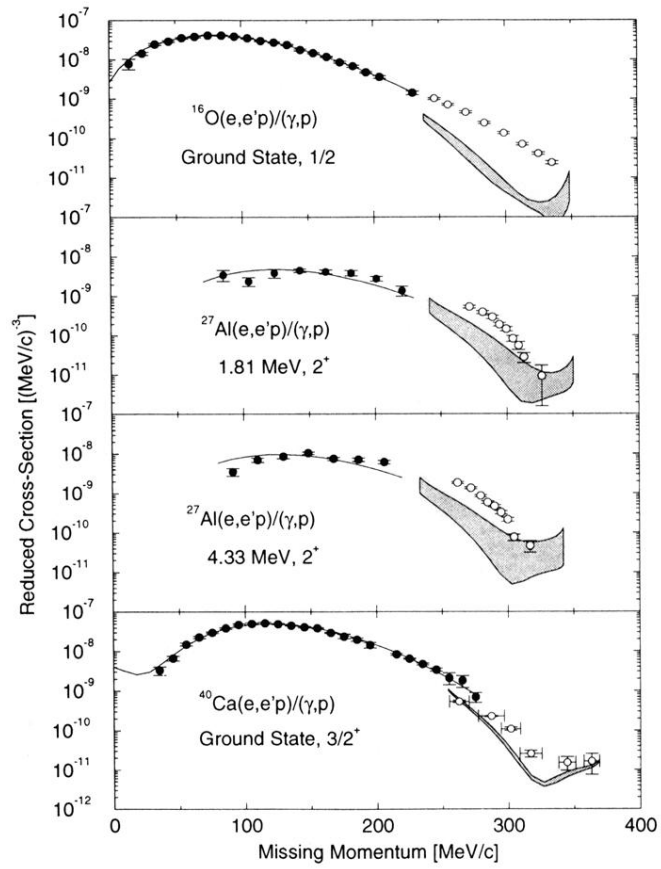
FIG. 2. Selected transitions for proton knockout from the nuclei ^{16}O, ^{27}Al, and ^{40}Ca. The points and curves have the same meanings as in Fig. 1.
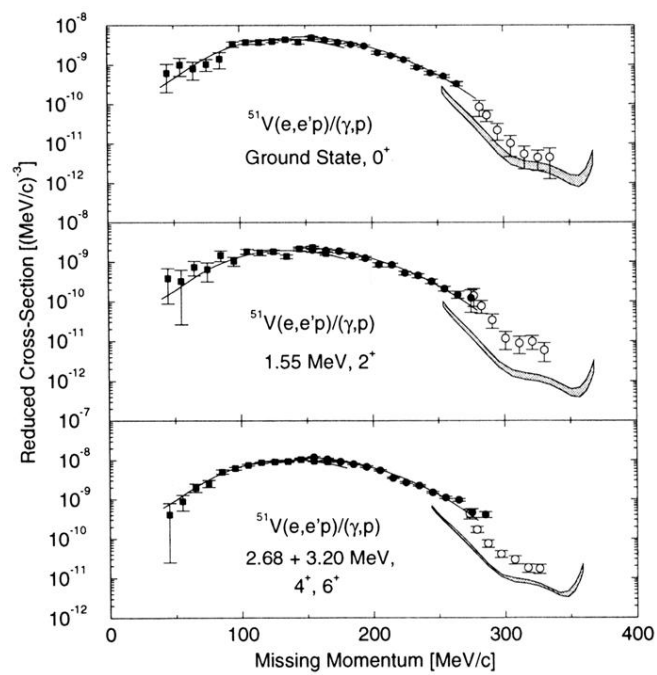
FIG. 3. The $1f_{7/2}$ transitions for proton knockout from ^{51}V. The points and curves have the same meanings as in Fig. 1. Note that in the third panel the sum of two transitions is shown.
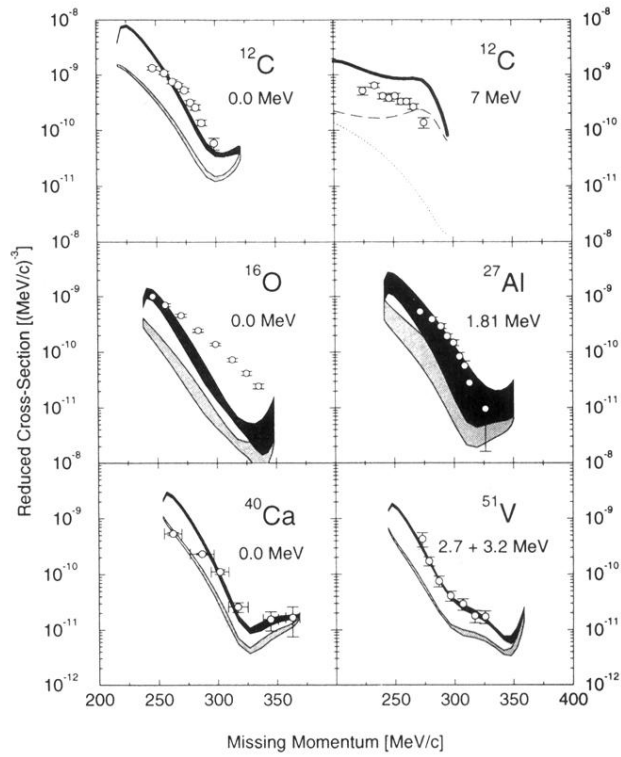
FIG. 4. The effect of applying the Siegert theorem to estimate MEC effects on some selected (γ, p) transitions. The DKO calculations are shown as light shaded bands, and the DKO+MEC calculations are represented by the darker bands. The $^{12}C(\gamma, p)$ transition to the 7 MeV complex is addressed separately in the text.